Altered Structural and Functional Connectivity in Large-Scale Neural Networks in Healthy Elderly with White Matter Hyperintensities

Natan Derek [*,1, a], Esin Avci-Colak[*,1, a], Riccardo Iandolo[2, a], Gitta Rohweder[a,b], Ioanna Sandvig[a], Axel Sandvig[*,a, c, d]

[1] E.A.C and N.D share first authorship.

[2] R. I. present address: TheraPanacea 7 bis boulevard Bourdon 75004 Paris – France

[a]*Department of Neuromedicine and Movement Science, Faculty of Medicine and Health Sciences, Norwegian University of Science and Technology (NTNU), Trondheim, Norway.*

[b] *Stroke Unit, Department of Medicine, St Olav's University Hospital, Trondheim, Norway.*

[c] *Department of Neurorehabilitation, Umeå University Hospital,Umeå, Sweden.*

[d]*Department of Community Medicine and Rehabilitation, Umeå University, Umeå, Sweden.*

[*] Corresponding authors: esin.avci@ntnu.no (E. Avci-Colak), axel.sandvig@ntnu.no (A. Sandvig) at Department of Neuromedicine and Movement Science, Edvard Griegs gate 8, 7030 Trondheim, Norway.

Clinical Trial Registration Information: The study is registered at *clinicaltrials.gov* with the *Project Identifier*: *NCT05086055.*

Abstract

White matter hyperintensities (WMH) are common neuroimaging findings in brain scans of elderly people. WMH lead to structural and functional changes in brain connectivity and impact cognitive function. Using 7T MRI, we examined 40 cognitively healthy subjects (16 females, mean age 69.3) with WMH presence, clustered into three groups of low, moderate, and high WMH burden. We used diffusion tensor imaging data to construct structural connectivity matrices and resting-state functional MRI data to construct functional connectivity matrices. Using network-based statistics (NBS) and graph-theory analysis (GTA), we compared the structural and functional network differences between the groups and their association to cognitive function. NBS analysis revealed altered structural connectivity strength in the default mode network (DMN) in the high WMH burden group, which correlated with the Trail Making Test scores. GTA revealed, that compared to the low burden, the high burden group had increased small-worldness and modularity in the structural connectivity, and increased assortativity in the functional connectivity. We found altered

betweenness centrality (BC) in the DMN on both structural and functional connectivity. The BC difference in the functional connectivity in the DMN between the high and the low WMH burden groups had a linear relationship with Montreal Cognitive Assessment scores. Our results demonstrate that WMH burden alters both structural and functional brain connectivity and affects large-scale network organization at local and global levels in an otherwise healthy elderly population.

Keywords: leukoaraiosis, graph theory analysis, network-based statistics, high resolution MRI

Introduction

White matter hyperintensities (WMH) are small lesions in the white matter, identified by T2-weighted brain magnetic resonance imaging (MRI)[1,2]. They are one of the most common structural changes associated with older age[3] and are linked to diseases like stroke, mild cognitive impairment, Alzheimer's disease and vascular dementias[1,4–9]. Investigation of the WMH-associated changes in the brain in cognitively healthy elderly individuals can provide insights into the WMH pathology itself and its implications for developing cognitive impairment.

WMH compromise the structural integrity of the brain and disrupt the communication between and within brain areas[10]. The impact of WMH on brain connectivity is two-fold. These lesions interrupt the white matter fiber tracts and damage the structural connections between brain regions[11]. Moreover, local and remote brain areas interact through large-scale networks and WMH can thus disrupt these functional connections[12]. MRI can non-invasively assess the large-scale structural and functional brain networks. Structural networks are visualized by diffusion tensor imaging (DTI) and studies have reported reduced structural connectivity (SC) strength and slower information processing in WMH patients[11,13]. The functional networks are assessed with functional MRI by measuring the temporally synchronized activation of blood-oxygen-level-dependent signals between different brain regions over time[14]. The resting-state functional networks, characterized by the repeated and coherent activation of widely distributed brain regions at rest[15,16], are reported to be affected by WMH[17,18]. WMH associated changes in functional connectivity (FC) are found within the default mode network, dorsal attention network, salience/ventral attention network and frontoparietal executive control network[19–23]. These functional networks are linked to cognition[24–26] and thus impairment in the large-scale neural connections is suggested to also disrupt the interaction of these networks, thereby impacting cognitive control and attention[27]. It has been shown that FC alterations due to WMH among these networks correlate with reduced processing speed, impaired memory function and reduced executive functioning[12,21,27–29]. Overall, the existing literature provides evidence that WMH change the structural and functional brain connectivity and impact cognitive function. However, it is still not fully understood how the pathological cascade induced by WMH disrupts the neural network so that it may cause progressive cognitive

impairment. Moreover, studies examining healthy elderly subjects with WMH typically focus on the functional connectivity, or the correlation between WMH burden and cognitive function[30–32]. Studies emphasizing both structural and functional connectivity in the same healthy elderly subjects are thus needed and may provide new insights as to how WMH lesions alter different communication modes in the brain and how these alterations relate to cognitive function.

In recent years, network-based statistics (NBS)[33] and graph theory analysis (GTA)[34] have been utilized as a means of exploring the large-scale structural and functional brain connectivity. Both methods model neural connections as a graph and construct a connectivity matrix by defining the neuronal ensembles as “nodes”, and the white matter fiber tracts as “edges”. For the FC matrix, edges are defined as the temporal co-activation of different regions[33,34]. NBS can help identify the network differences i.e., the strength of the network connection, and GTA allows to study the global and local characteristics of the networks, for example by providing different types of information on the number of neural connections in the network[34]. To the best of our knowledge, few studies have utilized NBS and GTA together to extensively study the different structural and functional connectivity modes at local and global levels using subject-specific DTI and resting-state functional MRI (rs-fMRI) in a sample of cognitively healthy elderly with WMH.

In this study we aimed to identify and compare the unique topological and large-scale functional network characteristics of a healthy elderly sample with high, moderate, and low WMH burdens. We applied NBS to identify the differences in structural and functional connectivity strength between the different burden groups based, respectively, on the DTI and rs-fMRI data. Next, we utilized GTA to construct whole-brain SC and FC matrices and the corresponding large-scale brain networks for different WMH burden groups. We then investigated and compared the global and local network characteristics and tested potential associations with cognitive function, evaluated by Trail Making Test and Montreal Cognitive Assessment. We anticipated that the high WMH burden group would have decreased structural connectivity strength and altered network characteristics both at global and local levels compared to the low burden group and we would find associations with the cognitive test scores.

Methods

Participants

40 subjects (24 males; age 69.3 ± 7.3 years) signed informed consent, composing the control arm of a stroke project. The baseline characteristics are reported in our previous work[35]. Inclusion criteria followed as: 1) age 55-85 years; 2) no current or previous psychiatric/neurological/neurodegenerative disease or cognitive symptoms; 3) no brain tumor/neurotrauma; 4) no aphasia; 5) can provide informed consent; 6) can be scanned with 7T MRI. A designated senior medical doctor working in the Stroke Department finalized the inclusions.

The study followed the Declaration of Helsinki and was approved by the regional ethical committee of Central Norway (REK Number: 171264).

Cognitive assessments

A certified administrator conducted Montreal Cognitive Assessment (MoCA) Norwegian 8.1 version[36]. Subjects with ≤ 12 years of education were given one extra point. The Trail Making Test[37] (TMT) followed two parts: TMT-A including only randomly distributed numbers 1-25 and TMT-B including both randomly distributed numbers 1-13 and letters A-L. Scoring was based on the time to finish each test in seconds.

MRI data acquisition

We used MRI at 7T (Magnetom Terra, equipped with a Nova Medical Head Coil 1TX/32RX, Siemens Healthcare GmbH, Erlangen, Germany) for scanning. The process of mapping anatomical brain areas is explained in our previous work[35]. The DTI protocols were adapted from the Human Connectome Project[38], acquired with a high spatial resolution of 1.4 mm isotropic (TR/TE = 5600 ms/71.0 ms) with three different shells of b = 0, 1000 and 2000 s/mm2/. For the rs-fMRI, a full-brain coverage gradient-echo EPI sequence (100 slices; FOV = 198 x 198 x 150 mm; isotropic resolution = 1.5 x 1.5 x 1.5 mm; TR = 1.53 s; FA = 68°; TE = 21 ms; echo spacing = 0.77 ms; bandwidth = 1456 Hz/Px; partial-fourier = 6/8; SMS = 4; phase-encoding direction = anterior-posterior; 318 volumes) were collected. To implement susceptibility distortion correction during subsequent processing, four volumes with opposite phase-encoding direction (i.e., posterior-anterior) were acquired. During rs-fMRI, we instructed the participants to look at a black cross on a white screen and remain focused.

Structural preprocessing, WMH segmentation and subjects' partitioning

The preprocessing of the structural T1-weighted data, the corresponding WMH segmentation and subjects' partitioning into 3 clusters are explained in our previous work[35]. We performed the brain parcellation on the output obtained from FreeSurfer using the available online tool[39,40]. This parcellation process utilizes the Schaefer atlas[41], resulting in the overall division of the brain into 200 regions. The following sections explain the processes to construct the matrices of structural connectivity (SC) using DTI data and the functional connectivity (FC) using rs-fMRI data.

DTI

Figure 1 illustrates the WMH spatial distribution at 7T, DTI, and rs-fMRI preprocessing and analysis pipelines. We conducted the whole-brain tractography using FSL[42] and MRtrix[43] for all the DTI preprocessing steps. The data processing involved the raw nifti data conversion to the MRtrix-specific .mif format, denoising using TOPUP[44], correction of artifacts using EDDY[45], and bias field correction to ensure data quality. We then applied the ACT framework to segment the brain into cortical gray matter, subcortical gray matter, white matter and cerebrospinal fluid[46]. We aligned the

results with the T1-preprocessed image using FLIRT with 6 degrees of freedom and BBR options[47].

To begin the construction of the streamline, we performed spherical deconvolution on the multi-shell-multi-tissue data using "dwi2response" function[48] and we computed fiber orientation distributions (FODs) for grey matter, WM, and CSF using the "dwi2fod" function. After that, we carried out the normalization of the FODs. We generated 10 million streamlines with "tckgen," setting maximum and minimum lengths to 250 mm and 5 mm, respectively. To optimize the tractography results while preserving connectivity information, we employed the "tcksift2" algorithm[49]. Finally, we parcellated the resulting tractography data into 214 regions based on the Schaefer atlas[41], which includes 14 regions of interests added from the freesurfer[40] regions. We constructed the SC matrix to represent the connectivity strength between these regions.

Rs- fMRI

All the preprocessing steps were performed using fmriprep[50], explained in our previous work[35]. Additionally, the average of 214 regions used the individual parcellated atlas were generated using 315 time points of the bold signal[40].

For the construction of the brain network based on FC from rs-fMRI data, we employed the dpabinet tools[51]. By this approach, we created a correlation matrix using the Pearson correlation coefficient for 200 nodes. We used the connectivity matrix obtained from the DTI data using the weight conversion function from the Brain Connectivity Toolbox (BCT) for normalization[52]. We carried out the normalization process to ensure that the values in the FC matrix were within the range of 0 to 1 and achieve standardized comparisons during subsequent network analysis.

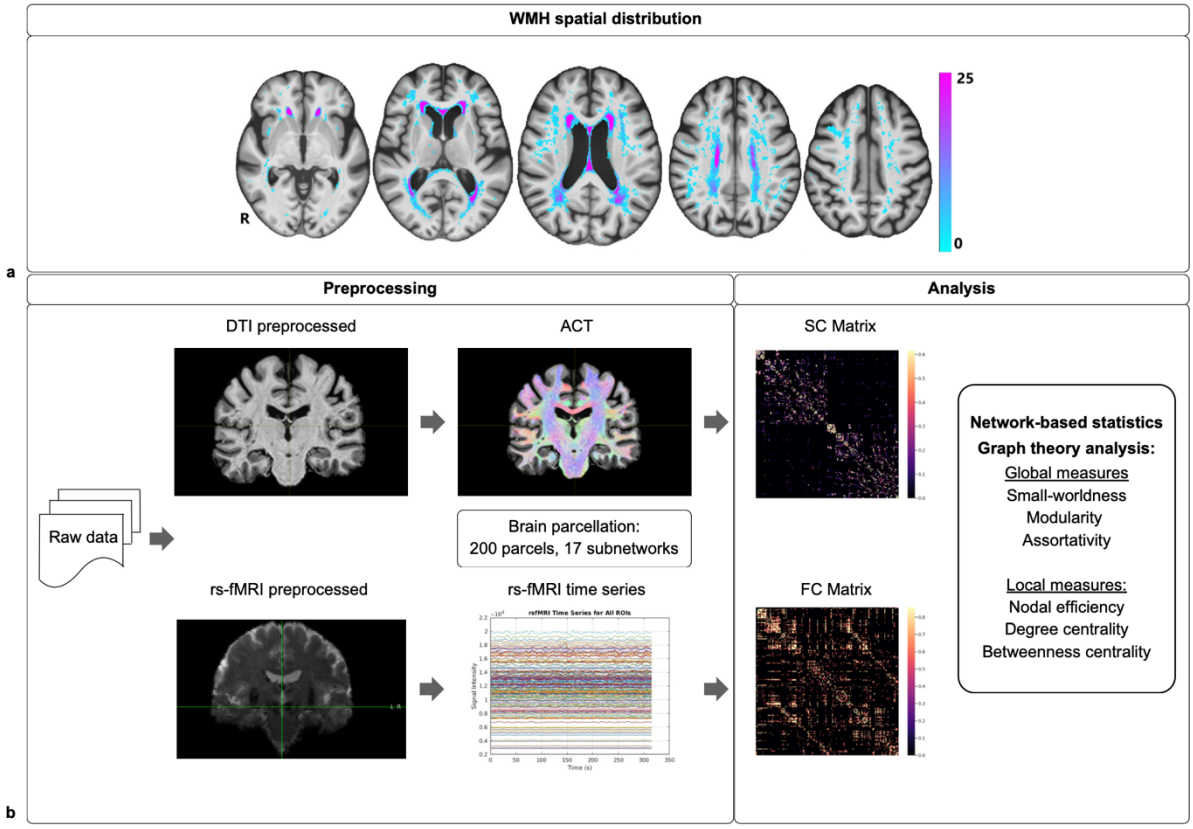

Figure 1. A. WMH spatial distribution at 7T, fractions of subjects in entire sample. Figure reused from Iandolo et al. (2024)[35] under the Creative Commons Attribution 4.0 International License (https://creativecommons.org/licenses/by/4.0/). **B.** DTI and rs-fMRI pipelines for MRI data preprocessing and analysis. Individual SC and FC matrices were constructed using NBS and GTA for the brain-network analysis. The nodes were generated based on Schaefer Atlas of 200 parcels and 17 networks[41]. *WMH: White matter hyperintensities, DTI: Diffusion tensor imaging, ACT: Anatomically-constraint tractography, SC: structural connectivity, rs-fMRI: resting state functional magnetic resonance imaging, FC: Functional connectivity, NBS: Network-based statistics, GTA: Graph theory analysis*

Network Analysis

Network-Based Statistics (NBS)

We employed network-based statistics (NBS) to assess intergroup differences in connectivity strength[33]. First, we performed two sample t-tests two-sided between each group (G1 compared to G2, G1 compared to G3, G2 compared to G3), followed by the permutation 5000 times according to PALM[53]. Then, we calculated the whole NBS results. A result of 200× 200 edges of t-statistics values were thresholded by an initial $P < 0.001$ as the output for each group comparison.

Graph Theory Analysis (GTA)

We applied the graph theory analysis (GTA) to further investigate network topologies and the differences between the groups[34]. We computed all the topological attributes under different sparsity ranges, varying from 0.01 to 0.5 (with an interval of 0.01). Then, we calculated the Area Under the Curve (AUC) for sparsity ranges from 0.1 to 0.34[54]. To calculate the small-worldness, random times was set to 100 as default. Following the same approach, for the two-sample t-tests, we performed PALM[53] to assess the differences between the groups on all the topological attribute measures.

For all GTA calculations, we used BCT[52] under the dpabinet toolbox[51]. We analyzed the brain network topology using multiple attributes: global level attributes of assortativity, clustering coefficient, average path length, modularity, and small-worldness; and the local level attributes of nodal efficiency, degree centrality and betweenness centrality for each individual node.

Statistical analysis

The correlation between significant edges identified in the NBS results and cognitive scales were analyzed using a significance level of FDR < 0.05 with the two-sample test permutation[51]. Ordinary least squares (OLS) regression was conducted for each clinical and cognitive measurement as independent variables to examine their individual relationships with both local and global properties, which served as the dependent variables. The analysis included an assessment of the relationships between these properties and proportional WMH calculated as the intracranial volume of the brain divided by total WMH, Age; scores of MoCA, TMT-A and TMT-B. For the between-group comparisons of local GTA properties, the non-parametric Mann-Whitney U test two-sided were used with the p value < 0.01.

Results

The demographic, clinical, cognitive and MRI characteristics of the cohort and WMH subgroups are reported in our previous work[35]. Briefly, we stratified 40 subjects according to their peripheral and deep WMH lesion burden using k-means clustering. Then we used the Calinski-Harabasz metric to quantify the groups with most within-clusters compactness and between-clusters separation[55], yielding 3 groups: Group 1 (G1) – low burden (low deep WMH and low-to-mild peripheral WMH), Group 2 (G2) – moderate burden (mild deep WMH and low-to-mild peripheral WMH), and Group 3 (G3) – high burden (heavy deep and peripheral WMH).

Structural connectivity strength differ between the high and the low WMH burden groups

We first investigated any differences in connectivity strength, assessed by edges, in the structural connectomes of the different WMH burden groups using NBS. We used the permutation-based p-value (Pperm) set at 0.001 to determine the statistical significance. Statistically significant differences between G1 and G3 were found (Fig. 2), and the dominant networks corresponding to

the significantly different edges included visual network VIS-A (16.2%), default mode network DMN-B (13.4%) and DMN-A (8.8%), and executive control network CON-B (13.1%) (Supplementary Fig. 1). We found a significant correlation between the edges of the DMN and VIS and the Trail Making Test–B (TMT-B) scores, corrected FDR < 0.05 (Supplementary Fig. 2). Statistically significant differences were further found between G2 and G3 (Supplementary Fig. 3). Additionally in the full sample of 40 subjects, we found a significant linear relationship for the Montreal Cognitive Assessment (MoCA) scores and the edges of VIS, DMN, salience/ventral attention network (SAL/VAN) and CON, corrected FDR < 0.05, indicating subjects with a higher MoCA scores had more connectivity strength in the edges corresponding to these networks (Supplementary Fig. 4). We found no significant difference for the FC data.

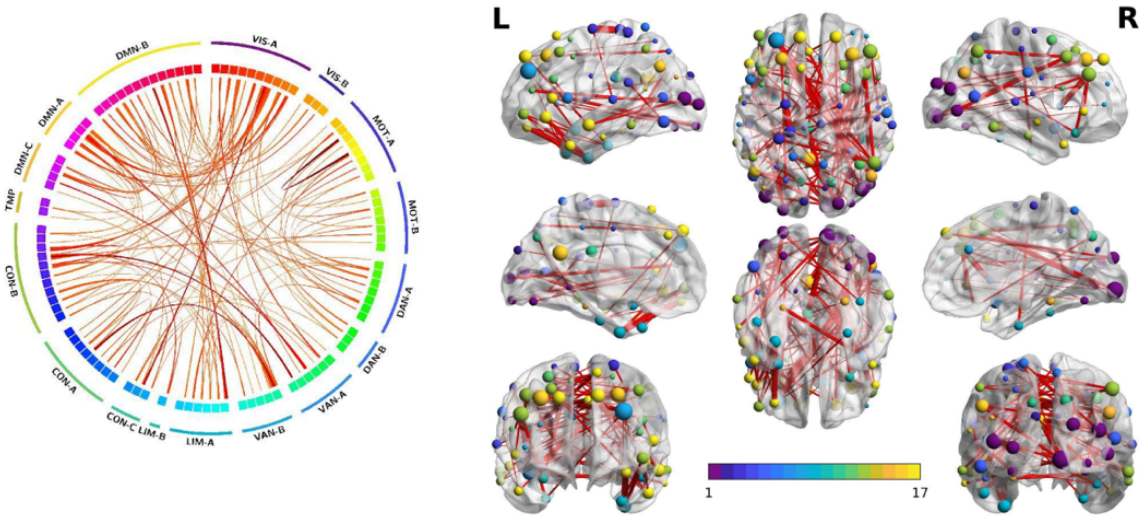

Figure 2. The edges with significantly different connectivity strengths identified by network-based statistics between G1 and G3 based on SC data. The node labels are grouped by the 17 Network Schaefer atlas[41], statistical significance p < 0.001. *G1 - low WMH burden group, G3 - high WMH burden group, SC: structural connectivity*

Structural and functional networks have different characteristics at global and local levels in the high- and low- WMH burden groups

We investigated and compared the global and local characteristics of the structural and functional networks for different WMH burden groups using GTA. On the global level, we compared the groups in terms of small-worldness, modularity and assortativity. On the local level, we compared the groups in terms of nodal efficiency (NE), degree centrality (DC) and betweenness centrality (BC). We used the permutation-based p-value (Pperm) set at 0.05 to determine the statistical significance.

Global network in the high WMH burden group has increased structural small-worldness, modularity, and assortativity, but decreased functional assortativity

We found significant differences in SC between G1 and G3 on Modularity_AUC (Pperm = 0.048), clustering coefficient Gamma_AUC (Pperm = 0.024) and SW parameter (Pperm = 0.03). Additionally, we found significant differences between G2 and G3 on Modularity_AUC (Pperm = 0.011) and Assortativity_AUC (Pperm = 0.056). In FC, we found significant differences between G1 and G3 in Assortativity_AUC (Pperm = 0.023) (Fig. 3).

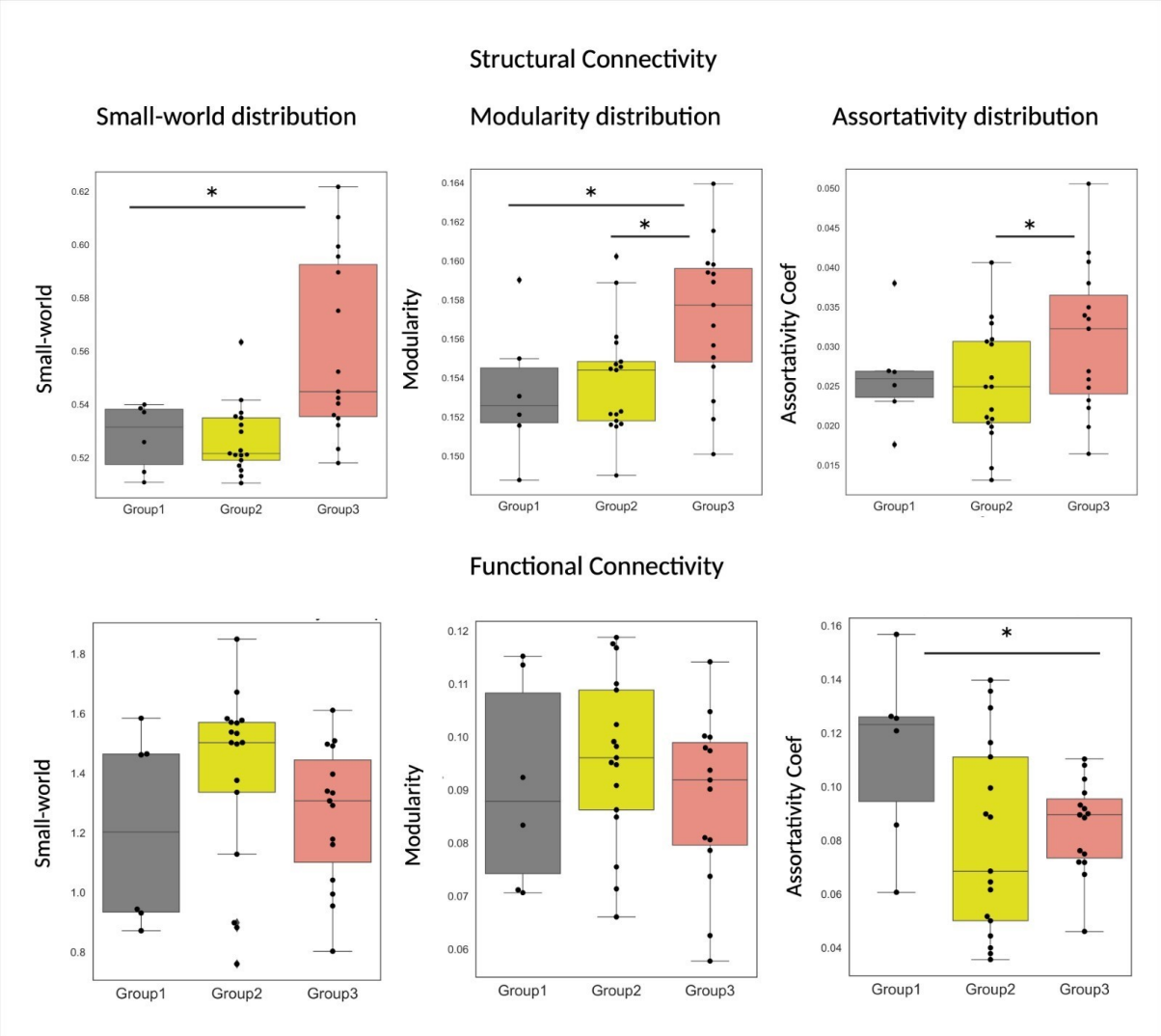

Fig. 3. Structural and functional connectivity global GTA differences among groups. Significant differences marked with an asterisk: For SC between G1 and G3 in small-worldness (Pperm = 0.03), modularity (Pperm = 0.048); between G2 and G3 in modularity (Pperm = 0.011), assortativity (Pperm = 0.056); for FC between G1 and G3 in assortativity (Pperm = 0.023). *SC: Structural connectivity, FC: Functional connectivity*

Additionally, we used OLS regression analysis to determine significant associations between the global GTA parameters and explanatory variables of mean connectivity strength, WMH proportion, age, MoCA scores, TMT-A scores and TMT-B scores. The significant and non-significant results are reported in Supplementary Table 1. Supplementary Fig. 5 depicts the linear associations between the explanatory variables and each global GTA variable for SC and FC individually.

Degree centrality and nodal efficiency are different between the high WMH burden and low WMH burden groups in large-scale functional neural networks

In SC, we found significant differences between G1 and G3 on BC corresponding to the edges of SAL/VAN-A, DMN-B, MOT-A and LIM-B ($p<0.01$). Between G1 and G2, we found significant differences on BC in the edges of DMN-B and LIM-B ($p<0.01$). Between G2 and G3, we found significant differences on BC in the nodes of MOT-A ($p<0.01$).

In FC, we found significant differences between G1 and G3 on BC corresponding to the edges of DMN-A and LIM-A($p<0.01$), on DC in the edges of DAN-A, SAL/VAN-A, VIS-A, VIS-B and MOT-A ($p<0.01$), on NE in the edges of VIS-B and MOT-B ($p<0.01$). Between G1 and G2, we found significant differences on DC in the edges of VIS-A and MOT-A ($p<0.01$). Between G2 and G3, we found significant differences on DC corresponding to the nodes of TMP ($p<0.01$).

The significant difference in FC on BC between G1 and G3 corresponding to edges of DMN-A was further found to have a significant linear association with the MoCA scores ($p=0.01$), indicating the difference in MoCA scores between these groups were reflected by the difference in betweenness centrality values among the edges of the DMN-A (Supplementary Fig. 6). We illustrated the BC difference along with the affected edges between G1 and G3 in Fig. 4 using spring layout[56], SC thresholded proportionally using BCT[52].

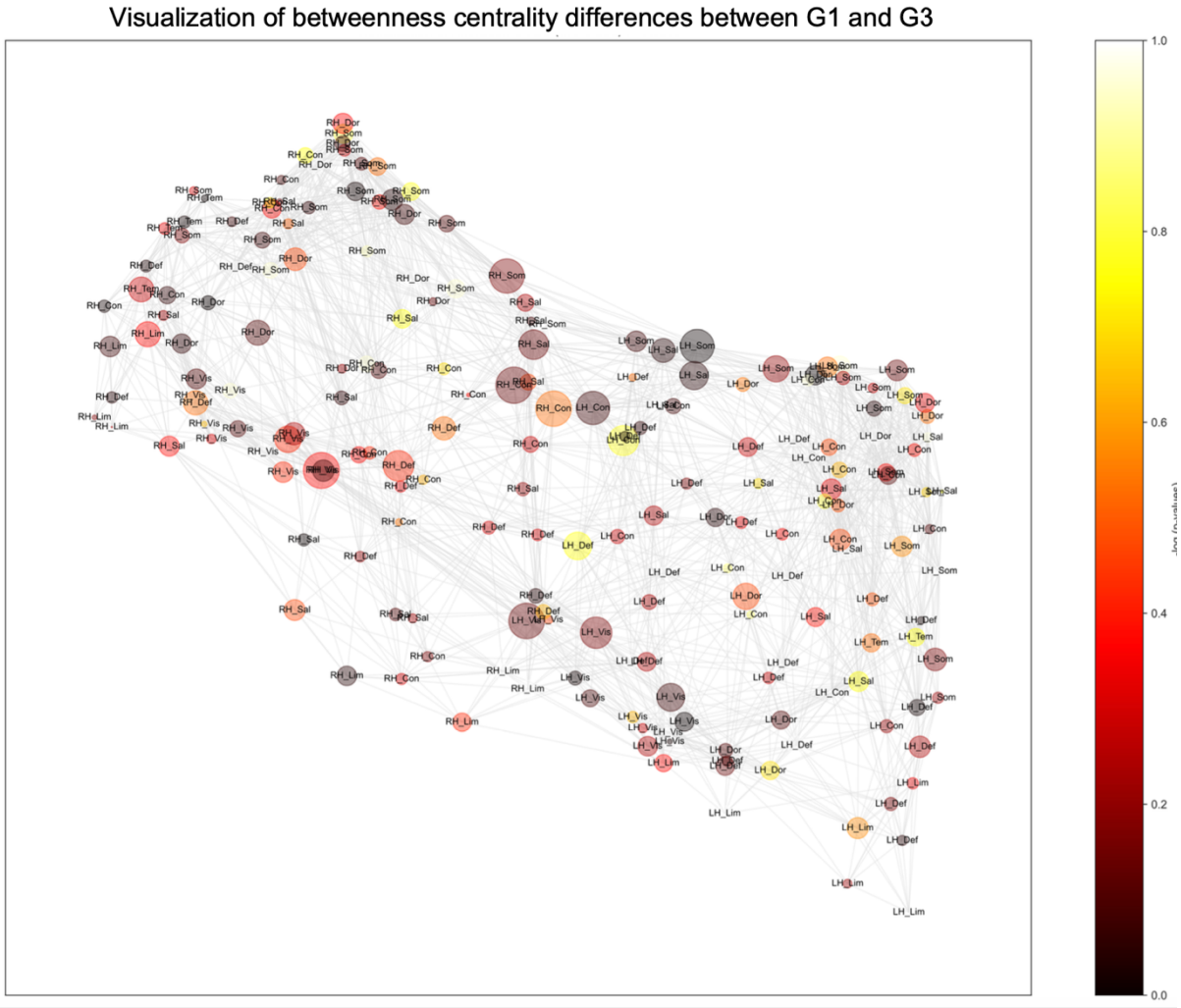

Figure 4. Illustration of the nodes and edges with their betweenness centrality (BC) values based on the structural connectome. The node sizes are based on the BC values of G1, and colors are based on the negative log p –values of the group differences. The labels of the nodes are taken from the Schaefer 17 subnetworks[41].

Secondly, by calculating the average of the 200 nodes and grouping them based on their indices into the corresponding 17 subnetworks[41], we illustrated how the local GTA properties differ between groups for the specific networks. Figure 5. A-C presents the SC and FC profiles of the three groups for NE, DC and BC based on these calculations. Fig. 5.D-F presents the whole-sample correlations of the subnetworks and WMH.

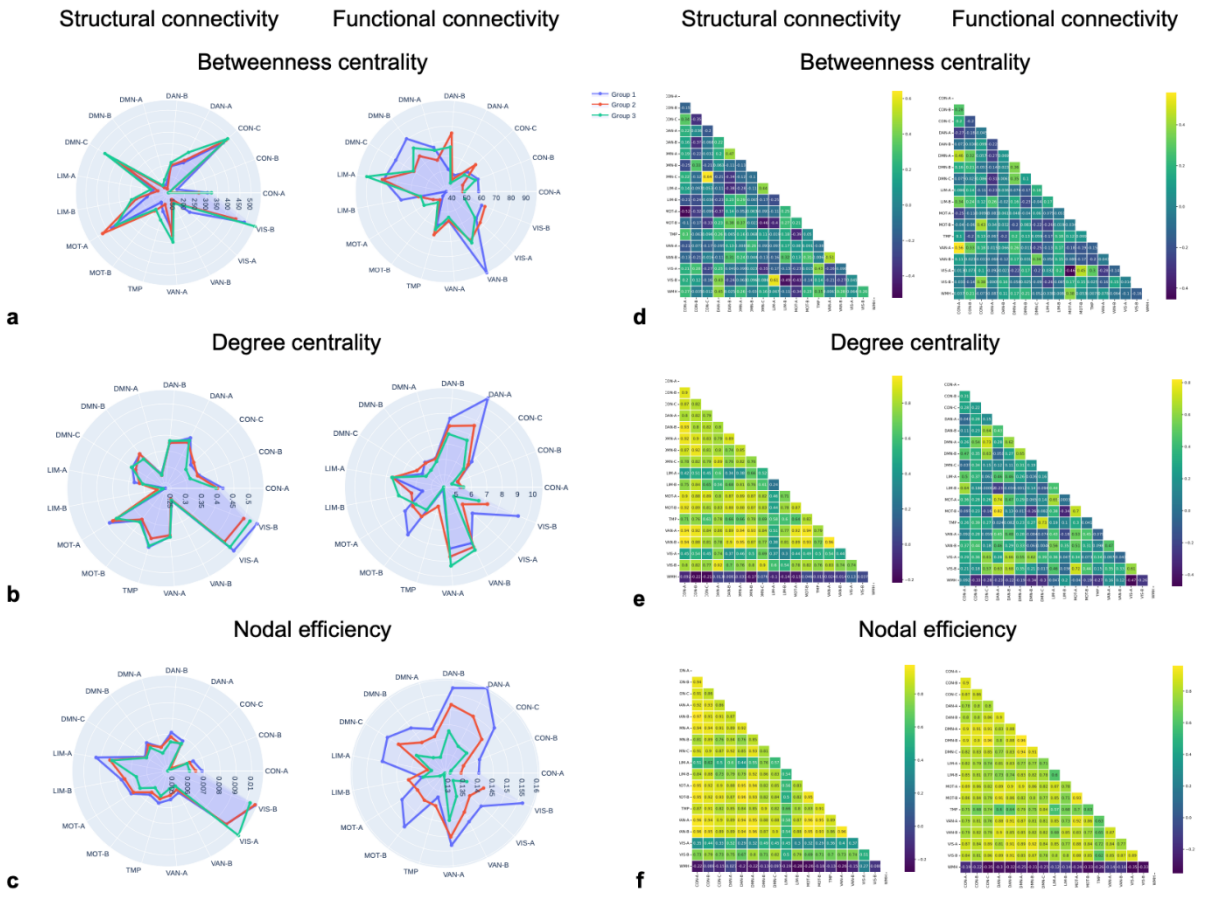

Figure 5. Average of network nodes grouped by the 17 subnetworks[41]. *Left columns: SC, Right columns: FC.* **A-C.** Network profiles for G1 (blue), G2 (red) and G3 (green). **D-F.** Correlation matrices for the whole sample and the subnetworks, last rows demonstrate WMH correlation. **A, D:** betweenness centrality. **B, E:** degree centrality. **C, F:** nodal efficiency. *SC: Structural connectivity, FC: Functional connectivity, WMH: White matter hyperintensities.*

Discussion

In this study, we investigated the structural and functional neural network characteristics of a sample of healthy elderly subjects without cognitive impairment. Within our sample, we compared three different groups with low (G1), moderate (G2) and high (G3) WMH burdens.

NBS analysis revealed that different WMH burdens were associated with different structural connectivity strength, and as we hypothesized the high WMH burden group had decreased connectivity strength. These connectivity strength differences were more pronounced between the high (G3) vs. low (G1) burden group, compared to the moderate (G2) vs. high (G3) burden group. This could indicate that WMH burden is increasingly reflected in the degenerative changes in the structural connectomes between the groups. The differences between G1 and G3 were most prominent in the areas corresponding to DMN structures and these edges that have different

structural connectivity strength demonstrated a correlation with the TMT-B scores as we hypothesized priorly. The TMT necessitates the engagement of multiple cognitive abilities by recruiting different brain regions[57–59], and part B further relies on the ability to modify answers and shift between different choices[60]. We found the difference in connectivity strength in the DMN-A network, which includes the areas of inferior parietal lobule, dorsal and medial prefrontal cortex (PFC), and posterior cingulate cortex (PCC). These areas have dense interactions with local and interregional brain areas[61]. Previous studies suggested that PCC connectivity within DMN were related to cognitive function[62,63] and that the structural integrity of dorsolateral PFC could be a contributing factor for healthy cognitive aging[64]. Increased WMH volume has been previously associated with reduction in cognitive function[17,19,30] and WMH load could predict the transformation from cognitively healthy to mild cognitive impairment[65,66]. The difference in connectivity strength between the high and low WMH burden groups in DMN areas correlating with the cognitive scores of TMT-B suggest that there could be a temporal relationship between the degree of WMH and increasing risk of gradual cognitive decline. WMH could thus represent an evolving pathological process, which in turn serve as a biomarker for the early stages of cognitive decline in otherwise healthy individuals.

Next, we investigated the global network characteristics of the low, moderate, and high WMH burden groups by GTA and as we expected, the high WMH burden group demonstrated altered network characteristics. We found clear structural differences, such that the high WMH burden group (G3) had higher small-worldness, modularity and longer average path length compared to the low WMH burden group (G1). Small-worldness is calculated as the clustering coefficient to average path length ratio. This metric thus indicates that G3 employed a longer distance to transfer information compared to G1, suggesting rerouting of information resulting from reduced structural integrity. A primary benefit of small-world organization in the brain is to decrease energy and wiring demands[67], by favoring low-cost, highly efficient pathways[68]. Damaged structural integrity in the neural network affects information transfer, which may result in rerouting through alternative nodal pathways. These additional connections could help improve efficiency within the network, however longer paths would also increase the metabolic costs such as the anatomical space needed for connections or the energy demand for information transfer[69]. It would also likely increase the time to accomplish the information transfer due to the overload of existing routes. One would further expect a higher error rate due to overload, which may not be consistent but dependent on the actual traffic at each timepoint. The increased energy demand for rerouting of information could have global consequences by shunting blood to areas with pathologically increased need for nutrient supply. Moreover, the higher modularity found in G3 suggests that this group had more densely connected modules with few external connections to the whole network, compared to both G1 and G2. Modularity has been suggested to promote adaptability and robustness[70]. For example, in response to abrupt local damage, existing modules can limit the impact to the region

where the damage occurs and rearrange the connections within the immediately affected module if it is necessary[70–72]. On the other hand, it has also been suggested that if modularity is too high, this may also affect communication and cooperation with other modules when needed[70]. Supporting these arguments, a previous PET-fMRI study found that the brain networks of Alzheimer's patients had higher modularity and assortativity compared to patients with mild cognitive impairment[73]. Our findings imply that structurally, G3 may have more reliance on the modular organization, since their average paths are longer and long-range communication is metabolically costly, thus, modules can promote neural communication within the network. On the other hand, G1 could utilize both the long-range connections and the modules, as the neural paths are shorter and more energy efficient, thus it can maintain interactions among different areas better compared to G3. We found that structurally the networks in the high WMH burden group (G3) were the most assortative, while functionally the networks in the low WMH burden group (G1) were the most assortative. Assortativity indicates that in a network, high-degree nodes tend to connect with other high-degree nodes, whereas low-degree nodes tend to connect with other low-degree nodes[74]. Previous research suggested that when a high-degree node gets damaged, other existing high-degree nodes connect to each other to prevent dysconnectivity in the overall network[75]. As such, higher assortativity in the network is beneficial in case of structural damage or loss of a specific node[75]. However, particularly for functionally interdependent networks, higher assortativity has been reported to negatively affect network stability and to decrease the speed of information propagation[75]. Clinical studies focusing on functional connectivity have reported that lower assortativity was found in Asperger's syndrome patients[76] and Alzheimer's patients[73,77] compared to control subjects, and they have discussed that the change in assortativity may be attributable to a more random brain network reconfiguration. Conversely, higher assortativity in structural connectivity has been reported for Alzheimer's patients compared to patients with mild cognitive impairment[79]. Similarly in our results, G3 presented structurally more assortative network organization, indicating high-degree nodes increased their connectivity with other high degree nodes, but as a result their network might have become less stable and slower. On the other hand, G1 presented functionally more assortative, indicating more stable network patterns and faster information transfer throughout the global network. It is also noteworthy that we have found significant linear associations with the TMT-B scores for all the global GTA measures on the structural connectome, suggesting the altered global network mechanisms impact the interaction of different brain regions, which is required during the cognitively demanding TMT-B task.

Lastly, we examined the local network characteristics of the different WMH burden groups. Structurally, we found alterations in the betweenness centrality between high (G3), moderate (G2), and low (G1) burden groups. In neural networks, some nodes are more important or "central" compared to others, and betweenness centrality helps determine through which nodes information is more likely to propagate[64]. Higher betweenness centrality indicates that there are not many

pathway options in the network and information must thus pass through the same central nodes at all times putting high demands on these nodes. On the other hand, lower betweenness centrality indicates that the network is well interconnected and there are several alternative route options through which information can pass[80]. As we hypothesized, we found that G3 had altered local network characteristics. G3 had significantly higher betweenness centrality within the structural network compared to both G2 and G1. G2 also had significantly higher betweenness centrality compared to G1, indicating that the interconnectedness of the networks gradually decreases with increasing WMH burden. Furthermore, both in the structural and functional connectomes, the betweenness centrality differences were found among the DMN nodes, while in the functional connectome, we also found a positive linear relationship with MoCA scores, showing that the subjects with higher cognitive test scores also had higher betweenness centrality on functional connectivity among these DMN regions. Alterations in betweenness centrality among DMN nodes were previously reported for different patient cohorts compared to healthy subjects on both structural and functional connectivity. One study compared the structural connectomes of three groups i.e., WMH patients with mild cognitive impairment, WMH patients without mild cognitive impairment and healthy controls and reported betweenness centrality differences among DMN nodes along with a mediatory effect of betweenness centrality on the relationship between language function and WMH[81]**.** Another study investigated the functional connectomes of patients with cerebral small vessel disease and healthy controls and reported betweenness centrality differences among DMN nodes, further correlated with attention[82]. In the present study, we found that the high WMH burden group had both structurally and functionally altered BC among the nodes of DMN, but we only found a correlation with MoCA scores on the functional connectome. Our results demonstrate that the network of the high WMH burden group (G3) interconnected differently compared to the low WMH burden group (G1) particularly among the DMN nodes. The higher MoCA scores in the low WMH burden group (G1) showing a correlation with the functional betweenness centrality among the DMN nodes might be due to G1 having more alternative pathways to propagate information, whereas the high burden group (G3) with lower MoCA scores may have limited number of central nodes they could recruit among DMN nodes.

Regarding the functional local network characteristics, we found differences between all groups for the degree centrality measure. Degree centrality is a measure of how strongly a node is connected to all the other nodes based on its direct connections[83]. We found that G3 had increased degree centrality among salience/ventral attention network (SAL/VAN) nodes, while G1 had increased degree centrality among dorsal attention network (DAN) nodes. Previous rs-fMRI studies have reported distinct functional connectivity patterns for DAN and SAL/VAN, but also a dynamic interaction between them based on task demand[84,85]. Rs-fMRI protocols commonly entail sustained and focused attention, which is suggested to relate to the activation of DAN, whereas SAL/VAN may take part in reorientation of attention in the presence of a salient stimulus[84,86]. Our

results suggest that G1 had more direct connections among nodes of DAN, which would potentially help successfully activate this network during rest-state fMRI protocol. On the other hand, in G3, the direct connections of several nodes may be disrupted due to WMH, possibly leading to the additional recruitment of SAL/VAN during the same protocol. The increased activation in SAL/VAN has also been previously reported to correlate with WMH load and it has been suggested to be a neuroplasticity mechanism, such that the increased activation could be a compensation towards WMH burden[87]. Lastly, we found a decrease in local nodal efficiency for G3 compared to G1. It has been previously reported that a decrease in local nodal efficiency can be associated with a higher WMH burden[88,89]. Our finding may thus suggest that G1 has more efficient neural communication because of less WMH impact on the functional network organization.

Conclusion

To summarize, our results demonstrated altered structural and functional connectivity associated with different WMH burdens in a cohort of healthy elderly. Compared to the low WMH burden, the high WMH burden group had both structural and functional differences in the global network and the local network. Altered DMN organization between the low WMH burden and high WMH burden groups having a correlation with cognitive test scores indicate that the interaction of brain areas during a cognitive task are affected by WMH burden. These results suggest that WMH lead to different communication modes in the brain networks of healthy elderly. Future studies can investigate WMH-related connectivity differences in patient cohorts i.e. small vessel disease patients and healthy subjects to establish the clinical application of WMH as an early marker for impending gradual cognitive decline.

CrediT Authorship Contribution Statement

Conceptualization: E.A.C., N.D., G.R., I.S., A.S., **Methodology:** E.A.C., N.D., R.I., G.R., I.S., A.S., **Software:** N.D., R.I., **Formal analysis:** N.D., **Investigation:** E.A., **Resources:** E.A.C., N.D., G.R., **Data curation:** E.A.C, N.D., R.I., **Writing – original draft:** E.A.C., N.D., **Writing – review & editing:** R.I., G.R., I.S., A.S., **Visualization:** E.A.C., N.D., **Supervision:** G.R., I.S., A.S., **Project administration:** A.S., **Funding acquisition:** A.S.

Declaration of competing interest

The authors declare no competing interests.

Data availability

Raw and processed MRI data that have been used are confidential. Other data will be made available upon reasonable request.

Acknowledgement:

We thank our study nurses Davide Vår Hauge and Torill Margrethe Saether for their invaluable help in the testing of the study subjects. We also thank the St. Olav's Hospital staff, the 7T MR Center and the Departement of Neuromedicine and Movement Science, NTNU for their collaboration. Lastly, we acknowledge financial support from: Samarbeidsorganet, Helse-Midt Norge (HMN), NTNU - Clinical Academic Group for Alzheimer's disease, Grant number 5981, and The Research Council of Norway - PROTEQT Grant number: 302523.

References

1. Prins, N. D. & Scheltens, P. White matter hyperintensities, cognitive impairment and dementia: an update. *Nature Reviews Neurology* **11**, 157–165 (2015).
2. Wardlaw, J. M., Valdés Hernández, M. C. & Muñoz-Maniega, S. What are White Matter Hyperintensities Made of?: Relevance to Vascular Cognitive Impairment. *JAHA* **4**, e001140 (2015).
3. Habes, M. *et al.* White matter lesions: Spatial heterogeneity, links to risk factors, cognition, genetics, and atrophy. *Neurology* **91**, e964–e975 (2018).
4. Aamodt, E. B. *et al.* Predicting the Emergence of Major Neurocognitive Disorder Within Three Months After a Stroke. *Front. Aging Neurosci.* **13**, 705889 (2021).
5. Botz, J., Lohner, V. & Schirmer, M. D. Spatial Patterns of White Matter Hyperintensities: A Systematic Review. *medRxiv* 2002–2023 (2023).
6. Debette, S. & Markus, H. S. The clinical importance of white matter hyperintensities on brain magnetic resonance imaging: systematic review and meta-analysis. *BMJ* **341**, c3666–c3666 (2010).
7. Epstein, A. *et al.* Chronic Covert Brain Infarctions and White Matter Hyperintensities in Patients With Stroke, Transient Ischemic Attack, and Stroke Mimic. *JAHA* **11**, e024191 (2022).
8. Giese, A.-K. *et al.* White matter hyperintensity burden in acute stroke patients differs by ischemic stroke subtype. *Neurology* **95**, (2020).
9. Hu, H.-Y. *et al.* White matter hyperintensities and risks of cognitive impairment and dementia: A systematic review and meta-analysis of 36 prospective studies. *Neuroscience & Biobehavioral Reviews* **120**, 16–27 (2021).

10. Langen, C. D. *et al.* White matter lesions relate to tract-specific reductions in functional connectivity. *Neurobiology of Aging* **51**, 97–103 (2017).
11. Vergoossen, L. W. M. *et al.* Interplay of White Matter Hyperintensities, Cerebral Networks, and Cognitive Function in an Adult Population: Diffusion-Tensor Imaging in the Maastricht Study. *Radiology* **298**, 384–392 (2021).
12. Huang, C. *et al.* Altered dynamic functional network connectivity and topological organization variance in patients with white matter hyperintensities. *J of Neuroscience Research* jnr.25230 (2023) doi:10.1002/jnr.25230.
13. Yang, D. *et al.* Impaired Structural Network Properties Caused by White Matter Hyperintensity Related to Cognitive Decline. *Front. Neurol.* **11**, 250 (2020).
14. Van Den Heuvel, M. P. & Hulshoff Pol, H. E. Exploring the brain network: A review on resting-state fMRI functional connectivity. *European Neuropsychopharmacology* **20**, 519–534 (2010).
15. Damoiseaux, J. S. *et al.* Consistent resting-state networks across healthy subjects. *Proc. Natl. Acad. Sci. U.S.A.* **103**, 13848–13853 (2006).
16. Power, J. D. *et al.* Functional Network Organization of the Human Brain. *Neuron* **72**, 665–678 (2011).
17. Kantarovich, K. *et al.* White matter lesion load is associated with lower within- and greater between- network connectivity across older age. *Neurobiology of Aging* **112**, 170–180 (2022).
18. Sun, Y. *et al.* Abnormal functional connectivity in patients with vascular cognitive impairment, no dementia: A resting-state functional magnetic resonance imaging study. *Behavioural Brain Research* **223**, 388–394 (2011).
19. Benson, G. *et al.* Functional connectivity in cognitive control networks mitigates the impact of white matter lesions in the elderly. *Alz Res Therapy* **10**, 109 (2018).
20. Ding, J.-R. *et al.* Altered connectivity patterns among resting state networks in patients with ischemic white matter lesions. *Brain Imaging and Behavior* **12**, 1239–1250 (2018).

21. Jaywant, A. *et al.* Estimated Regional White Matter Hyperintensity Burden, Resting State Functional Connectivity, and Cognitive Functions in Older Adults. *The American Journal of Geriatric Psychiatry* **30**, 269–280 (2022).
22. Kim, H. J. *et al.* Distinctive Resting State Network Disruptions Among Alzheimer's Disease, Subcortical Vascular Dementia, and Mixed Dementia Patients. *JAD* **50**, 709–718 (2016).
23. Liu, R. *et al.* Distinctive and Pervasive Alterations of Functional Brain Networks in Cerebral Small Vessel Disease with and without Cognitive Impairment. *Dement Geriatr Cogn Disord* **47**, 55–67 (2019).
24. Fornito, A., Harrison, B. J., Zalesky, A. & Simons, J. S. Competitive and cooperative dynamics of large-scale brain functional networks supporting recollection. *Proc. Natl. Acad. Sci. U.S.A.* **109**, 12788–12793 (2012).
25. Menon, V. Large-scale brain networks and psychopathology: a unifying triple network model. *Trends in Cognitive Sciences* **15**, 483–506 (2011).
26. Smallwood, J. *et al.* The default mode network in cognition: a topographical perspective. *Nat Rev Neurosci* **22**, 503–513 (2021).
27. Crockett, R. A. *et al.* Painting by lesions: White matter hyperintensities disrupt functional networks and global cognition. *Neuroimage* **236**, 118089 (2021).
28. Chen, X. *et al.* Disrupted functional and structural connectivity within default mode network contribute to WMH-related cognitive impairment. *NeuroImage: Clinical* **24**, 102088 (2019).
29. Liu, Y. *et al.* Different Dynamic Nodal Properties Contribute to Cognitive Impairment in Patients with White Matter Hyperintensities. *Brain Sciences* **12**, 1527 (2022).
30. Chavda, R., Cao, J. S. & Benge, J. F. Neuropsychological impact of white matter hyperintensities in older adults without dementia. *Applied Neuropsychology: Adult* **28**, 354–362 (2021).
31. Porcu, M. *et al.* The association between white matter hyperintensities, cognition and regional neural activity in healthy subjects. *Eur J of Neuroscience* **54**, 5427–5443 (2021).
32. Silbert, L. C., Howieson, D. B., Dodge, H. & Kaye, J. A. Cognitive impairment risk: White matter hyperintensity progression matters. *Neurology* **73**, 120–125 (2009).

33. Zalesky, A., Fornito, A. & Bullmore, E. T. Network-based statistic: Identifying differences in brain networks. *NeuroImage* **53**, 1197–1207 (2010).
34. Bullmore, E. & Sporns, O. Complex brain networks: graph theoretical analysis of structural and functional systems. *Nat Rev Neurosci* **10**, 186–198 (2009).
35. Iandolo, R. *et al.* Characterizing upper extremity fine motor function in the presence of white matter hyperintensities: A 7 T MRI cross-sectional study in older adults. *NeuroImage: Clinical* **41**, 103569 (2024).
36. Nasreddine, Z. S. *et al.* The Montreal Cognitive Assessment, MoCA: A Brief Screening Tool For Mild Cognitive Impairment: MOCA: A BRIEF SCREENING TOOL FOR MCI. *Journal of the American Geriatrics Society* **53**, 695–699 (2005).
37. Partington, J. E. & Leiter, R. G. Partington's Pathways Test. *Psychological Service Center Journal* **1**, 11–20 (1949).
38. Vu, A. T. *et al.* High resolution whole brain diffusion imaging at 7T for the Human Connectome Project. *Neuroimage* **122**, 318–331 (2015).
39. Dale, A. M., Fischl, B. & Sereno, M. I. Cortical surface-based analysis: I. Segmentation and surface reconstruction. *Neuroimage* **9**, 179–194 (1999).
40. Faskowitz, J. faskowit/multiAtlasTT v0.0.1. Zenodo https://doi.org/10.5281/ZENODO.4459737 (2021).
41. Schaefer, A. *et al.* Local-global parcellation of the human cerebral cortex from intrinsic functional connectivity MRI. *Cerebral cortex* **28**, 3095–3114 (2018).
42. Jenkinson, M., Beckmann, C. F., Behrens, T. E. J., Woolrich, M. W. & Smith, S. M. Fsl. *Neuroimage* **62**, 782–790 (2012).
43. Tournier, J.-D. *et al.* MRtrix3: A fast, flexible and open software framework for medical image processing and visualisation. *NeuroImage* **202**, 116137 (2019).
44. Andersson, J. L. R., Skare, S. & Ashburner, J. How to correct susceptibility distortions in spin-echo echo-planar images: application to diffusion tensor imaging. *NeuroImage* **20**, 870–888 (2003).

45. Andersson, J. L. R. & Sotiropoulos, S. N. An integrated approach to correction for off-resonance effects and subject movement in diffusion MR imaging. *NeuroImage* **125**, 1063–1078 (2016).
46. Smith, R. E., Tournier, J.-D., Calamante, F. & Connelly, A. Anatomically-constrained tractography: Improved diffusion MRI streamlines tractography through effective use of anatomical information. *NeuroImage* **62**, 1924–1938 (2012).
47. Jenkinson, M., Bannister, P., Brady, M. & Smith, S. Improved Optimization for the Robust and Accurate Linear Registration and Motion Correction of Brain Images. *NeuroImage* **17**, 825–841 (2002).
48. Dhollander, T., Raffelt, D. & Connelly, A. Unsupervised 3-tissue response function estimation from single-shell or multi-shell diffusion MR data without a co-registered T1 image. in vol. pp. 5 (Lisbon, Portugal, 2016).
49. Smith, R. E., Tournier, J.-D., Calamante, F. & Connelly, A. SIFT2: Enabling dense quantitative assessment of brain white matter connectivity using streamlines tractography. *NeuroImage* **119**, 338–351 (2015).
50. Esteban, O. *et al.* fMRIPrep: a robust preprocessing pipeline for functional MRI. *Nature methods* **16**, 111–116 (2019).
51. Yan, C.-G., Wang, X.-D., Zuo, X.-N. & Zang, Y.-F. DPABI: Data Processing & Analysis for (Resting-State) Brain Imaging. *Neuroinform* **14**, 339–351 (2016).
52. Rubinov, M. & Sporns, O. Complex network measures of brain connectivity: Uses and interpretations. *NeuroImage* **52**, 1059–1069 (2010).
53. Winkler, A. M., Ridgway, G. R., Webster, M. A., Smith, S. M. & Nichols, T. E. Permutation inference for the general linear model. *NeuroImage* **92**, 381–397 (2014).
54. Yang, H. *et al.* Disrupted intrinsic functional brain topology in patients with major depressive disorder. *Mol Psychiatry* **26**, 7363–7371 (2021).
55. Liu, Y., Li, Z., Xiong, H., Gao, X. & Wu, J. Understanding of internal clustering validation measures. in *2010 IEEE international conference on data mining* 911–916 (IEEE, 2010).

56. Hagberg, A. A., Schult, D. A. & Swart, P. J. Exploring Network Structure, Dynamics, and Function using NetworkX. in *Proceedings of the 7th Python in Science conference* (eds. Varoquaux, G., Vaught, T. & Millman, J.) 11–15 (2008).
57. Gjellesvik, T. I. *et al.* Effects of High-Intensity Interval Training After Stroke (The HIIT Stroke Study) on Physical and Cognitive Function: A Multicenter Randomized Controlled Trial. *Archives of Physical Medicine and Rehabilitation* **102**, 1683–1691 (2021).
58. Oosterman, J. M. *et al.* Assessing mental flexibility: neuroanatomical and neuropsychological correlates of the trail making test in elderly people. *The Clinical Neuropsychologist* **24**, 203–219 (2010).
59. Zakzanis, K. K., Mraz, R. & Graham, S. J. An fMRI study of the Trail Making Test. *Neuropsychologia* **43**, 1878–1886 (2005).
60. Pérez-Parra, J. E. & Restrepo-de-Mejía, F. The Trail Making Test (part B) is associated with working memory: A concurrent validity study. *Applied Neuropsychology: Adult* 1–9 (2023) doi:10.1080/23279095.2023.2171793.
61. Braga, R. M., DiNicola, L. M. & Buckner, R. L. *Situating the Left-Lateralized Language Network in the Broader Organization of Multiple Specialized Large-Scale Distributed Networks*. http://biorxiv.org/lookup/doi/10.1101/2019.12.11.873174 (2019) doi:10.1101/2019.12.11.873174.
62. Leech, R. & Sharp, D. J. The role of the posterior cingulate cortex in cognition and disease. *Brain* **137**, 12–32 (2014).
63. Leech, R., Braga, R. & Sharp, D. J. Echoes of the Brain within the Posterior Cingulate Cortex. *J. Neurosci.* **32**, 215–222 (2012).
64. Evangelista, N. D. *et al.* Independent Contributions of Dorsolateral Prefrontal Structure and Function to Working Memory in Healthy Older Adults. *Cerebral Cortex* **31**, 1732–1743 (2021).
65. Smith, E. E. *et al.* Magnetic Resonance Imaging White Matter Hyperintensities and Brain Volume in the Prediction of Mild Cognitive Impairment and Dementia. *Arch Neurol* **65**, (2008).

66. Boyle, P. A. *et al.* White matter hyperintensities, incident mild cognitive impairment, and cognitive decline in old age. *Ann Clin Transl Neurol* **3**, 791–800 (2016).
67. Bassett, D. S. & Bullmore, E. Small-World Brain Networks. *Neuroscientist* **12**, 512–523 (2006).
68. Latora, V. & Marchiori, M. Economic small-world behavior in weighted networks. *Eur. Phys. J. B* **32**, 249–263 (2003).
69. Bassett, D. S. *et al.* Cognitive fitness of cost-efficient brain functional networks. *Proc. Natl. Acad. Sci. U.S.A.* **106**, 11747–11752 (2009).
70. Sporns, O. & Betzel, R. F. Modular Brain Networks. *Annu. Rev. Psychol.* **67**, 613–640 (2016).
71. Kashtan, N. & Alon, U. Spontaneous evolution of modularity and network motifs. *Proc. Natl. Acad. Sci. U.S.A.* **102**, 13773–13778 (2005).
72. Kashtan, N., Noor, E. & Alon, U. Varying environments can speed up evolution. *Proc. Natl. Acad. Sci. U.S.A.* **104**, 13711–13716 (2007).
73. Khokhar, S. K. *et al.* Alzheimer's disease is associated with increased modularity and assortativity: Evidence from structural and metabolic connectivity. *Alzheimer's & Dementia* **19**, e075199 (2023).
74. Lim, S., Radicchi, F., Van Den Heuvel, M. P. & Sporns, O. Discordant attributes of structural and functional brain connectivity in a two-layer multiplex network. *Sci Rep* **9**, 2885 (2019).
75. Noldus, R. & Van Mieghem, P. Assortativity in complex networks. *jcomplexnetw* **3**, 507–542 (2015).
76. Javaheripour, N. *et al.* Altered brain network organization in adults with Asperger's syndrome: decreased connectome transitivity and assortativity with increased global efficiency. *Front. Psychiatry* **14**, 1223147 (2023).
77. Khokhar, S. K. *et al.* Alzheimer's Disease Is Associated with Increased Network Assortativity: Evidence from Metabolic Connectivity. *Brain Connect* **13**, 610–620 (2023).
78. Bahrami, M. & Hossein-Zadeh, G.-A. Assortativity changes in Alzheimer's diesease: A resting-state FMRI study. in *2015 23rd Iranian Conference on Electrical Engineering* 141–144 (IEEE, Tehran, Iran, 2015). doi:10.1109/IranianCEE.2015.7146198.

79. Khokhar, S. K. *et al.* Alzheimer's disease is associated with increased modularity and assortativity: Evidence from structural and metabolic connectivity. *Alzheimer's & Dementia* **19**, e075199 (2023).
80. Butz, M., Steenbuck, I. D. & Van Ooyen, A. Homeostatic structural plasticity increases the efficiency of small-world networks. *Front. Synaptic Neurosci.* **6**, (2014).
81. Chen, H. *et al.* Altered morphological connectivity mediated white matter hyperintensity-related cognitive impairment. *Brain Research Bulletin* **202**, 110714 (2023).
82. Xin, H. *et al.* Disrupted topological organization of resting-state functional brain networks in cerebral small vessel disease. *Human Brain Mapping* **43**, 2607–2620 (2022).
83. Cañete-Massé, C. *et al.* Abnormal degree centrality and functional connectivity in Down syndrome: A resting-state fMRI study. *International Journal of Clinical and Health Psychology* **23**, 100341 (2023).
84. Fox, M. D., Corbetta, M., Snyder, A. Z., Vincent, J. L. & Raichle, M. E. Spontaneous neuronal activity distinguishes human dorsal and ventral attention systems. *Proc. Natl. Acad. Sci. U.S.A.* **103**, 10046–10051 (2006).
85. Vossel, S., Geng, J. J. & Fink, G. R. Dorsal and Ventral Attention Systems: Distinct Neural Circuits but Collaborative Roles. *Neuroscientist* **20**, 150–159 (2014).
86. Seeley, W. W. *et al.* Dissociable Intrinsic Connectivity Networks for Salience Processing and Executive Control. *J. Neurosci.* **27**, 2349–2356 (2007).
87. De Marco, M., Manca, R., Mitolo, M. & Venneri, A. White Matter Hyperintensity Load Modulates Brain Morphometry and Brain Connectivity in Healthy Adults: A Neuroplastic Mechanism? *Neural Plasticity* **2017**, 1–10 (2017).
88. Wang, Y. *et al.* Impaired functional network properties contribute to white matter hyperintensity related cognitive decline in patients with cerebral small vessel disease. *BMC Med Imaging* **22**, 40 (2022).
89. Zheng, W. *et al.* Metabolic syndrome-related cognitive impairment with white matter hyperintensities and functional network analysis. *Obesity* **31**, 2557–2567 (2023).